Inclusions Elimination and Resistivity Restoration of CdTe:Cl Crystals by Two-Step Annealing

Marek Bugár, Eduard Belas, Roman Grill, Jan Procházka, Štěpán Uxa, Pavel Hlídek, Jan Franc, Roman Fesh, and Pavel Höschl

***Abstract*—The aim of this work was to find an effective annealing treatment leading to a complete elimination of Te inclusions and simultaneously to conservation of the resistivity of CdTe:Cl crystals with varying chlorine doping level. This goal was reached by an application of two post-growth annealing steps. The first annealing step performed under Cd overpressure led to a significant reduction of Te inclusions. However, Cd-rich thermal treatment converted crystals into high-conductive n-types and re-annealing of the material in a Te atmosphere was necessary to restore the material resistivity. After application of the second annealing step under Te overpressure, resistivity higher than 10^8 Ωcm was observed only in samples with high chlorine doping levels of $n_{Cl} \approx 2 \times 10^{17}$ cm^{-3}. In addition, a new emission at 1.26 eV was observed in the photoluminescence spectra after two-step annealing. The size of Te inclusions, resistivity, photoluminescence spectra and detection properties of CdTe:Cl crystals before and after the two-step thermal treatment are discussed.**

***Index Terms*—Annealing, CdTe, inclusions, resistivity.**

I. Introduction

HIGH-RESISTIVE materials based on CdTe, especially CdZnTe:In and CdTe:Cl, are widely used for preparation of X-ray and gamma-ray detectors working at room temperature. The quality of detectors is strongly affected by the presence of structural defects within the material, especially Te inclusions [1]. Te-rich inclusions behave as trapping centers for electrons and significantly decrease the charge collection efficiency (CCE). An effective technological step towards reducing the size of Te inclusions is a post-growth annealing of the crystal in a Cd atmosphere [2], [3]. However, such a thermal treatment leads to a marked decrease of the material resistivity below 10^8 Ωcm and to loss of its detection ability. On the other hand, an annealing of the detector-grade CdTe:Cl under argon overpressure in the temperature range 400–550°C slightly enhances the material resistivity, but reduces the size of inclusions only partly [4], [5]. Hence, this work is focused on finding of optimal annealing conditions ensuring the inclusion elimination and the high-resistivity preservation. The annealing treatment is performed in two annealing steps. The first annealing step under Cd pressure is focused on an effective reduction of Te inclusions. The second step performed under Te pressure is aimed at finding of annealing conditions resulting in a resistivity enhancement and suppression of the new second phase defects formation. Beside Te inclusions and resistivity, also the photoluminescence (PL) spectra as well as gamma-ray and alpha-particle spectroscopy of samples are investigated before and after two-step annealing.

Manuscript received December 15, 2010; revised March 17, 2011 and May 16, 2011; accepted June 05, 2011. Date of publication July 12, 2011; date of current version August 17, 2011. This work is a part of research plan MSM 0021620834 by the Ministry of Education of the Czech Republic and supported in part by the Grant Agency of the Czech Republic under Contracts 102/09/H074 and 102/10/0148, the Grant Agency of the Charles University under Contract 135710, and by Grant SVV-2010-261306.

The authors are with the Institute of Physics, Charles University, Prague CZ-121 16, Czech Republic (e-mail: bugar@karlov.mff.cuni.cz; belas@karlov.mff.cuni.cz; grill@karlov.mff.cuni.cz; jan.prochazka@mff.cuni.cz; uxa@karlov.mff.cuni.cz; pavel.hlidek@mff.cuni.cz; franc@karlov.mff.cuni.cz; fesh@karlov.mff.cuni.cz; hoschl@karlov.mff.cuni.cz).

Digital Object Identifier 10.1109/TNS.2011.2159394

II. Experimental

CdTe:Cl samples from two different vendors were used. One crystal ingot grown by the Vertical Gradient Freeze (VGF) technique using 6N starting materials was prepared at the Institute of Physics at Charles University. Samples with dimensions of $5 \times 5 \times 2.5$ mm^3 were cut from three different parts of the ingot with doping levels $n_{Cl}^{VGF-1} = 3.4 \times 10^{16}$ cm^{-3}, $n_{Cl}^{VGF-2} = 6.9 \times 10^{16}$ cm^{-3} and $n_{Cl}^{VGF-3} = 2 \times 10^{17}$ cm^{-3}. The doping level of the samples was established by measuring of the carrier concentration of samples annealed in Cd vapor, in which the donor Cl_{Te} was the dominant point defect. Six samples were prepared from each part of the ingot for two-step annealing experiments. Another set of 6 samples with dimensions of $5 \times 5 \times 2$ mm^3 was cut from a wafer prepared by the Traveling Heater Method (THM) produced by Acrorad Ltd. The chlorine concentration in THM samples was $n_{Cl}^{THM} = 2.4 \times 10^{17}$ cm^{-3}. Annealing was performed in an evacuated ampoule placed in a two-zone furnace. Before the annealing process, a quartz ampoule was etched in HF, cleaned by distilled water and dried in a dryer with low dustiness. Samples were put together with the metal source into the quartz ampoule, which was evacuated and sealed. 6N Cd/Te metals prepared by Nippon Ltd. were placed in the zone with lower temperature for the pressure control during the annealing. The temperature notation T_1/T_2 (e.g. 700/550°C) used in this paper represents the annealing temperature of the sample/vapor source, respectively. The resistivity of samples lower than 10^7 Ωcm was measured by Hall effect measurements using the Van der Pauw configuration. The resistivity higher than 10^7 Ωcm was determined by the contactless resistivity mapping equipment COREMA [6] due to a high leakage current observed during four-point contact Hall effect measurements. The type of conductivity was established in all samples based on Hall effect measurements. The density and the size of Te inclusions were determined by

0018-9499/$26.00 © 2011 IEEE

IR microscope with a resolution limit of $\sim 1.4\ \mu\mathrm{m}$. Photoluminescence spectra were obtained by a Bruker IFS 66S Fourier spectrometer using laser excitation sources at 632.8 nm (1.96 eV) and 795 nm (1.56 eV) and Si, Ge and InSb detectors. γ-ray and α-particle spectra were measured using an Amptec A250 charge-sensitive pre-amplifier, Ortec 671 amplifier and Ortec Easy-MCA multichannel analyzer. Gamma-ray spectra were measured on samples having planar electroless deposited Au contacts using an $^{241}\mathrm{Am}$ (59.5 keV) gamma-ray source. In case of an ideal charge collection, the energy of 59.5 keV corresponds to the 270th channel in the gamma-ray spectrum. The value of applied voltage on the detector was corrected with respect to the detector resistivity and the input resistance of the pre-amplifier. The $\mu\tau$-product of electrons was evaluated using an $^{241}\mathrm{Am}$ (5.49 MeV) α-particle source. In case of an ideal charge collection, the energy of 5.49 MeV corresponds to the 1150th channel in the alpha-particle spectrum. Between every technological step and measurement, all sample surfaces were mechanically polished, chemo-mechanically polished in 2% Br-ethyleneglycol solution and etched in 2% Br-methanol solution. An approximately 100 μm-thick surface layer was removed from the sample by described surface treatment after each annealing step. Additional 50 μm were removed after Hall effect and spectroscopic measurement to remove gold contacts. In all measurements the actual sample thickness was considered.

III. Results

A. As-Grown Crystals

Both investigated crystals contained a large density of Te inclusions with diameter up to 25 μm. VGF samples exhibited the p-type conductivity and the resistivity of $\rho^{VGF-1} = 3.3 \times 10^5\ \Omega\mathrm{cm}$, $\rho^{VGF-2} = 7 \times 10^7\ \Omega\mathrm{cm}$ and $\rho^{VGF-3} = 2 \times 10^9\ \Omega\mathrm{cm}$. It is expected that the sample resistivity was connected with the chlorine doping level [Cl]. Similar dependence of the material resistivity on [Cl] was found in [7], where high-resistive CdTe:Cl was obtained in crystals with $[\mathrm{Cl}] > 1 \times 10^{17}\ \mathrm{cm}^{-3}$. This can be explained based on the results of Meyer *et al.* [8], who showed, that in crystals with $[\mathrm{Cl}] < 1 \times 10^{17}\ \mathrm{cm}^{-3}$ the concentration of the dominant acceptor—chlorine A-center $\mathrm{Cl_{Te}} - \mathrm{V_{Cd}}$—exceeds the concentration of the dominant donor $\mathrm{Cl_{Te}}$ and the concentration of both dominant point defects is equal for $[\mathrm{Cl}] \approx 1 \times 10^{17}\ \mathrm{cm}^{-3}$. THM as-grown samples exhibited the n-type conductivity and $\rho^{THM} = 2 \times 10^9\ \Omega\mathrm{cm}$.

B. Annealing in Cd Vapor

The annealing step in Cd vapor, which reduces the size of Te inclusions, was performed on all investigated samples. Cd-rich annealing at 700/600°C for 24 hours, as proposed by [3], was found to be not sufficient for the inclusions reduction for VGF samples. This was probably caused by an enhanced concentration of impurities present in the as-grown VGF crystal and recognized by an increased amount of peaks present in the region of bound excitons in PL spectra (see Fig. 4) leading to slower diffusion processes in the material. Finally, it was found out that

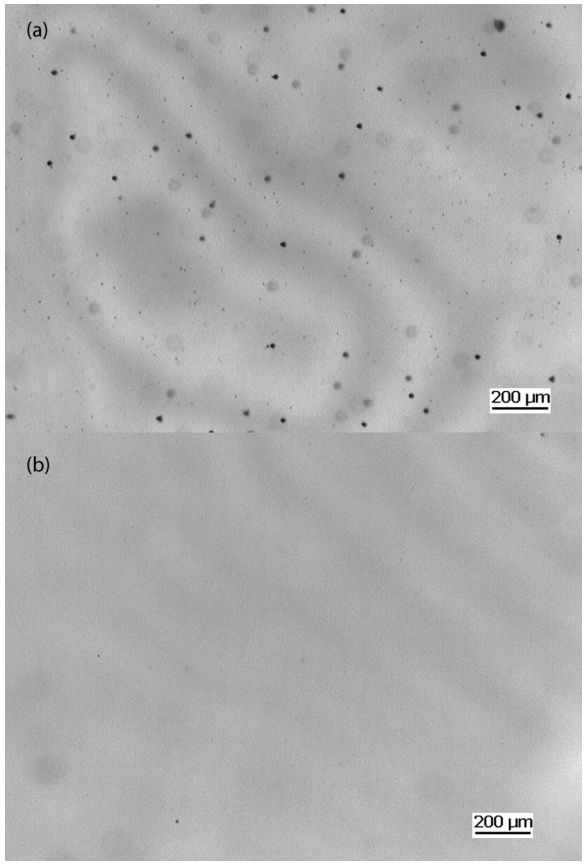

Fig. 1. IR microscope image of the same area in VGF sample (a) before and (b) after two-step annealing.

the Cd-rich annealing at 800/750°C for 24 hours with a cooling rate of $0.8°\mathrm{C/min}$. effectively reduced the size of Te inclusions to sizes below 3 μm (Fig. 1) and this annealing treatment was applied to all investigated VGF samples. On the other hand, Te inclusions in THM samples were completely eliminated by a thermal treatment at 700/600°C for 24 hours with a cooling rate of $0.8°\mathrm{C/min}$. (Fig. 2).

An adverse consequence of the Cd-rich annealing was a significant decrease of the resistivity of samples from both crystals to $\rho < 0.1\ \Omega\mathrm{cm}$. All annealed samples exhibited the n-type conductivity. This result can be explained by an annihilation of $\mathrm{V_{Cd}}$ by in-diffusion of $\mathrm{Cd_I}$ into the crystal during the Cd-rich annealing, which leads to a loss of the compensation and to setting the donor $\mathrm{Cl_{Te}}$ as the dominant point defect.

Hall effect measurements performed on samples annealed in Cd vapor were used for evaluation of the chlorine concentration [Cl] in the samples. Cd-rich annealing conditions used for the chlorine content [Cl] determination were the same as for the inclusion elimination. We assume that [Cl] dominates above both—the concentration of cadmium vacancies $[\mathrm{V_{Cd}}]$ and all unintentionally dopped impurities—so that $\mathrm{n} = [\mathrm{Cl}]$ may be applied. Since the chlorine atoms are incorporated in the tellurium sublattice, we expect that the concentration of chlorine in the crystal lattice is affected by annealing in Cd vapor only slightly. Moreover, a redistribution of impurities [9] from Te inclusions into the crystal lattice may occur during the Cd-rich annealing.

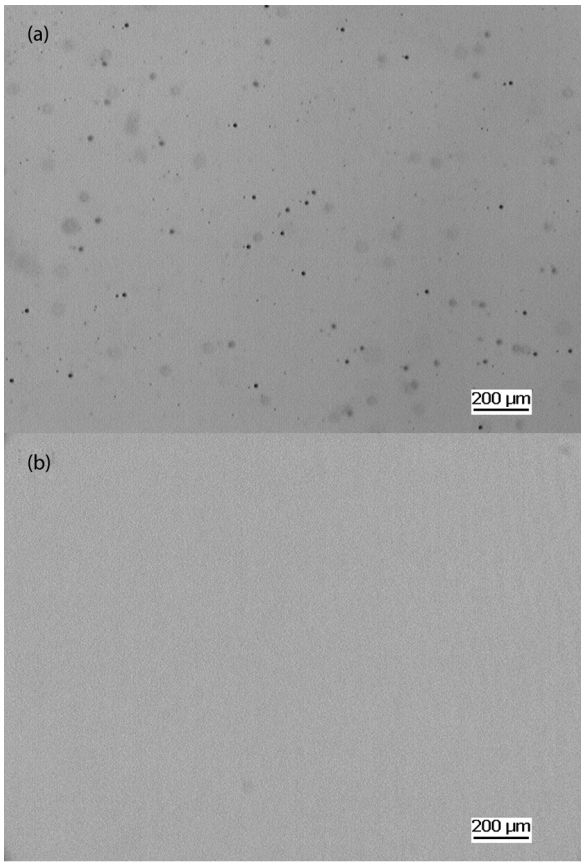

Fig. 2. IR microscope image of the same area in THM sample (a) before and (b) after two-step annealing.

C. Re-Annealing in Te Vapor

The aim of the second annealing step in a Te atmosphere was to increase the concentration of acceptors $(\mathrm{V_{Cd}}, \mathrm{Cl_{Te}} - \mathrm{V_{Cd}})$ close to the concentration of the dominant donor $\mathrm{Cl_{Te}}$ resulting in an increase of the material resistivity. Generally, during the annealing in Te vapor native shallow acceptors $(\mathrm{V_{Cd}}, \mathrm{V_{Cd}} - \mathrm{Cl_{Te}})$ together with native donors $(\mathrm{Te_{Cd}})$ are formed with concentrations depending on the applied Te pressure [10]. When shallow donors $(\mathrm{Cl_{Te}})$ and acceptors ($\mathrm{V_{Cd}}$, chlorine A-center, most of impurities) are compensated, the position of the Fermi energy is pinned on a deep level close to the CdTe midgap and semi-insulating (SI) material is formed.

To find an optimal thermal treatment under Te pressure leading to increase of the material resistivity, a systematic investigation of Te-rich annealing conditions was performed. Samples from three parts of the VGF ingot and samples from the THM wafer were pre-annealed in a Cd atmosphere and re-annealed in Te vapor at various pressures. The resistivity of samples after the second annealing step under Te overpressure is plotted in Fig. 3. The resistivity of all samples pre-annealed in Cd vapor significantly increased after their re-annealing in a Te atmosphere. From three types of VGF samples, the highest resistivity was achieved in VGF-3 samples. The resistivity of VGF-1 and VGF-2 samples after two-step annealing did not reach the initial resistivity and was over one order of magnitude lower. On the other hand, the resistivity restoration back to $\rho = 2 \times 10^9\ \Omega\mathrm{cm}$ of VGF-3 samples was observed after two-step annealing. Te-rich annealing of VGF samples at 700°C for 24 hours with the temperature of the Te source in the range 550–600°C was found to be optimal concerning the annealing time, sample resistivity, sample homogeneity and negligible sample sublimation. The cooling rate after the annealing was kept lower than $1^\circ\mathrm{C/min}$. with the aim to suppress of Te precipitates formation [11], [12]. The size of the created Te precipitates was below the resolution limit of the IR microscopy. Most of samples exhibited the p-type conductivity, only one VGF-3 sample annealed at the lowest Te pressure was n-type (in Fig. 3 labeled by a dotted square).

THM samples were annealed in Te vapor at 700°C at various Te pressures for 24 hours with a cooling rate of $0.8^\circ\mathrm{C/min}$. After the two-step annealing, no Te precipitates visible by IR microscopy were observed. The final resistivity of samples did not reach the initial resistivity of as-grown material and was in the range $\rho = 5 - 9 \times 10^8\ \Omega\mathrm{cm}$ depending on the applied Te overpressure. The highest resistivity was observed after the annealing at 700/540°C for 24 hours. All annealed THM samples exhibited the p-type conductivity. To prove the reproducibility of the two-step annealing treatment, two THM samples were always annealed together in the same Te-rich annealing run. After the annealing, their mutual difference of the resistivity was below 30%.

VGF-1, VGF-2 and THM samples exhibited after two-step annealing lower resistivity than before the annealing treatment. The reason for this effect is not clear at this time. It is difficult to decide, whether it was caused by a contamination of the material during the annealing process or whether this phenomenon rather had a physical origin.

From results, plotted in Fig. 3, can be concluded that the final resistivity of the samples was determined mainly by the chlorine doping concentration and was practically independent of the applied Te pressure $\mathrm{P_{Te2}}$ during the second Te-rich re-annealing. The observed weak pressure dependence can be explained by two models:

a) it is expected that the dynamic processes concern mainly the Cd sublattice in CdTe, where the volatile Cd may be easily removed from the lattice and the formation energy of the relevant point defects is low [13]. The defect density at Cd sublattice is determined by the partial Cd pressure $\mathrm{P_{Cd}}$ linked to $\mathrm{P_{Te2}}$ via the reaction constant $K_i(T)$ [14]

$$P_{Cd} = K_i(T)/\sqrt{P_{Te2}}. \tag{1}$$

In an ideal case of an isothermal annealing at thermal equilibrium the sample temperature $\mathrm{T} = \mathrm{T_1}$ should be used for the calculation of the reaction constant $K_i(T)$. At the two-zone furnace annealing, however, the component pressures are ruled by the cold zone temperature $\mathrm{T} = \mathrm{T_2}$ where Te is disposed. Consequently, $\mathrm{P_{Cd}}$ in a two-zone furnace at Te annealing can be significantly reduced and, moreover, the cooling/heating of the Te source does not entail the usually expected increase/decrease of $\mathrm{P_{Cd}}$ according (1), even an opposite course is obtained. The value of $\mathrm{P_{Cd}}$ becomes more doubtful, if pure Te in the cold zone is used. In that case $\mathrm{P_{Cd}}$ near the sample is set

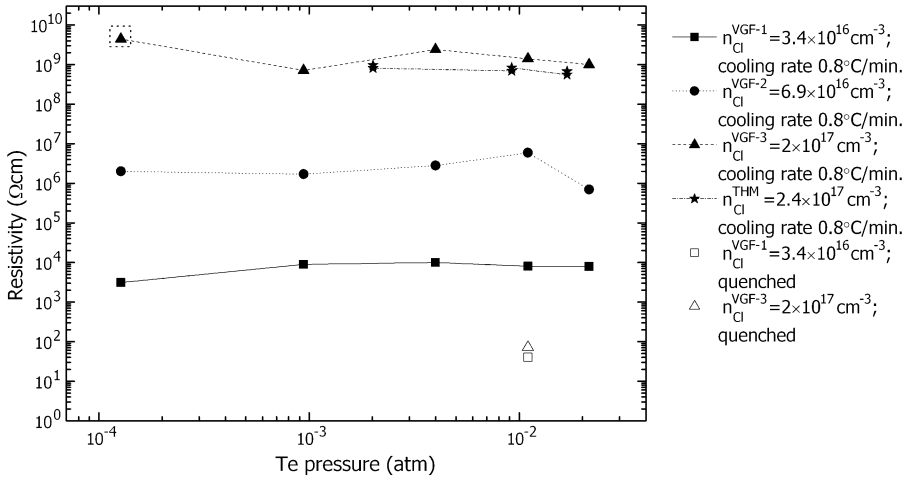

Fig. 3. The dependence of resistivity on Te overpressure after the second annealing step in Te vapor. Every point represents the resistivity of one sample after two-step annealing. Most of the samples were annealed at 700°C for 24 hours. Samples annealed at the lowest Te pressure 1.26×10^{-4} atm were annealed at 600°C for 50 hours. Filled symbols are samples cooled slowly after the second Te-rich annealing. Empty symbols represent samples quenched in the air after the second Te-rich annealing step. Lines are guides for eyes only.

by highly unspecific dynamic process of the evaporation of Cd from the sample, Cd flux toward the cold zone and dissolution in Te. Such methodological shortcomings of the two-zone annealing can result in the conductivity apparently independent on Te pressure. Final properties of the material depend only slightly on applied Te pressure at Te-rich annealing and the process resembles rather the annealing in vacuum than the annealing at defined pressures.

b) the second explanation can be based on a compensation process occuring during the Te-rich annealing concerning shallow donors $\mathrm{Cl_{Te}}$ and acceptors $\mathrm{V_{Cd}}$ and $\mathrm{Cl_{Te}} - \mathrm{V_{Cd}}$. During the Te-rich annealing $[\mathrm{V_{Cd}}]$ is set at elevated value. During slow post-anneal cooling, Cd vacancies form with $\mathrm{Cl_{Te}}$ the chlorine A-centers, whose concentration is determined by [Cl]. With decreasing temperature, $\mathrm{V_{Cd}}$ start to precipitate or vanish on extended defects and $[\mathrm{V_{Cd}}]$ decreases. Therefore, the concentration of acceptors is given mainly by chlorine A-centers and depends more on the chlorine doping level than on the applied Te pressure during the Te-rich annealing.

The first model can be indirectly supported by results from "*in-situ*" high-temperature Hall effect measurements of undoped CdTe and CdTe:In performed under Te overpressure [12], where only weak pressure dependence of the conductivity and Hall constant was observed during the measurements at 700°C. Contrary to this, to prove the second suggested model, one VGF-1 and one VGF-3 sample was cooled down rapidly in the air after the second Te-rich annealing step. Both samples, in Fig. 3 plotted as empty symbols, exhibited low resistivity ($\rho_{quenched}^{VGF-1} = 40\ \Omega\mathrm{cm}$ and $\rho_{quenched}^{VGF-3} = 72\ \Omega\mathrm{cm}$) and the p-type conductivity. We suppose that during the fast cooling $\mathrm{V_{Cd}}$ mainly remain "frozen" in the crystal lattice or start to create precipitates and a formation of chlorine A-centers is not dominant. This leads to an increased concentration of acceptor defects (mainly $[\mathrm{V_{Cd}}]$) compared to $[\mathrm{Cl_{Te}}]$ and low-resistive p-type material is obtained. This experiment supports the idea that the compensation occurs during the cooling of the material and is based mainly on the compensation of the donor $\mathrm{Cl_{Te}}$ and the acceptor chlorine A-center. To conclude, both models seem to have an experimental rationale, however, it is difficult to decide, which model explains the weak pressure dependence of the resistivity after two-step annealing more accurately.

High-resistive CdTe:Cl usually exhibits the p-type conductivity compared to CdTe:In with typical n-type conductivity [12]. This phenomenon can be explained by a compensation model concerning dominant point defects—doping donors ($\mathrm{In_{Cd}}$ or $\mathrm{Cl_{Te}}$) and acceptors ($\mathrm{V_{Cd}}$; $\mathrm{In_{Cd}} - \mathrm{V_{Cd}}$ or $\mathrm{Cl_{Te}} - \mathrm{V_{Cd}}$) [15]. Within this model, the position of the Fermi energy is given by the relation:

$$\mu_F = \frac{1}{2}\left(f(T,p) + E_{V_{Cd}} + E_A + E_i^{V_{Cd}} + E_i^A\right) \qquad (2)$$

where $f(T,p)$ is a function depending on temperature and pressure of the system; $E_{V_{Cd}}$ and E_A is the formation energy of cadmium vacancy and A-center, respectively; and $E_i^{V_{Cd}}$ and E_i^A is the ionization energy of $\mathrm{V_{Cd}}$ and A-center, respectively. The parameters E_A and E_i^A depend on the composition of an A-center. For crystals doped by indium $E_A = -0.3$ eV and $E_i^A = 140$ meV [16] can be used. In chlorine doped crystals $E_A = -0.5$ eV and $E_i^A = 120$ meV [16]. Based on (2), the position of the Fermi level in CdTe:Cl is shifted approximately 110 meV closer to the valence band in comparison with CdTe:In crystals. Therefore, high-resistive chlorine doped CdTe exhibits usually the p-type conductivity and high-resistive CdTe:In is typically n-type.

From the obtained results, it can be concluded that the chlorine doping level is the most important parameter determining whether CdTe:Cl crystal is high-resistive ($\rho > 10^8\ \Omega\mathrm{cm}$) after two-step annealing or not. This effect can be explained by a

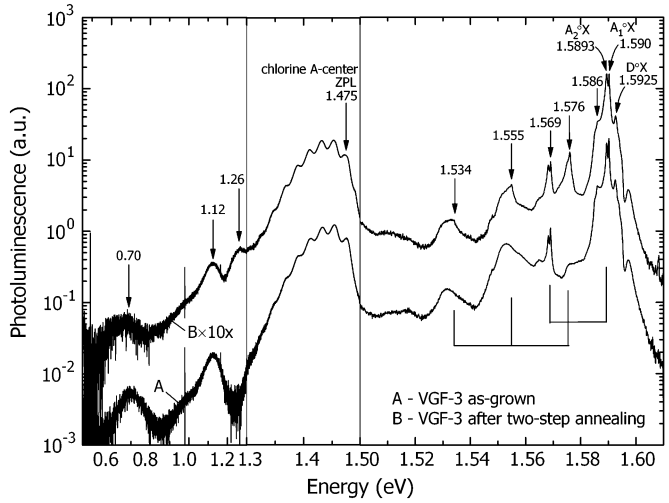

Fig. 4. PL spectra of VGF-3 samples before and after two-step annealing. Peak intensity at 1.576 eV increased and emission at 1.26 eV appeared after two-step annealing.

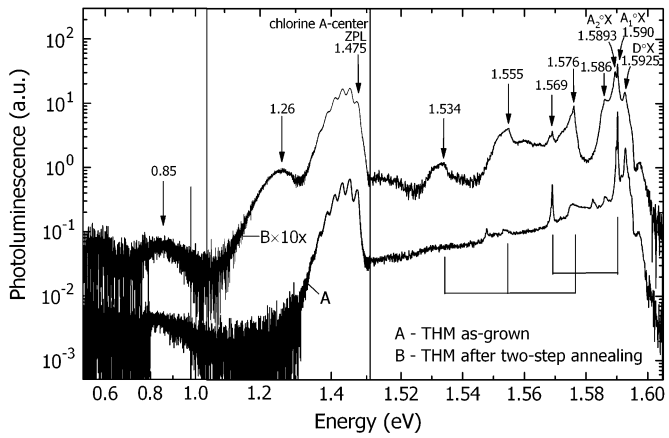

Fig. 5. PL spectra of THM samples before and after two-step annealing. Similarly to annealed VGF-3 samples, PL structures at 1.576 eV and 1.26 eV appeared in THM samples after two-step annealing.

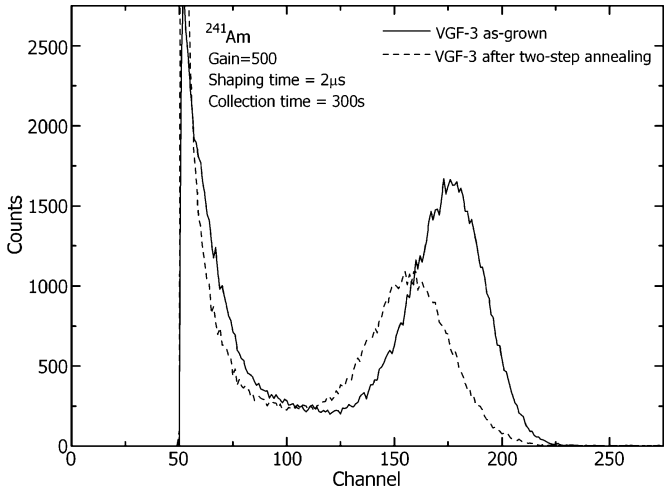

Fig. 6. Gamma-ray spectra of VGF-3 sample before and after two-step annealing. Spectra were measured at 250 V.

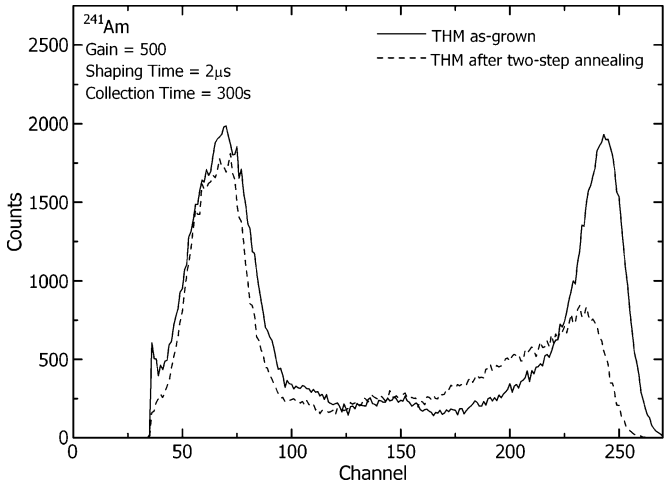

Fig. 7. Gamma-ray spectra of THM sample before and after two-step annealing. Spectra were collected at 250 V.

compensation model based on the compensation of the donor $\mathrm{Cl_{Te}}$ and the acceptor chlorine A-center. Our experiments and also results of Ohmori *et al.* [7] and Meyer *et al.* [8] lead to the conclusion that good compensation occurs in the CdTe:Cl material with chlorine doping level above $10^{17}\ \mathrm{cm^{-3}}$.

D. Photoluminescence Spectra

PL spectra of VGF-3 (Fig. 4) and THM (Fig. 5) samples before and after two-step annealing were measured in the energy range of 0.5–1.62 eV. Two significant changes were observed in annealed samples. The first was an increase of the peak intensity at 1.576 eV; the second effect was a creation of a non-standard emission at 1.26 eV. In earlier PL studies [17], [18], a similar emission at about 1.27 eV was observed in Au doped CdTe. In Hamann's work [17], a broad peak at 1.27 eV was found. Molva *et al.* [18] observed a structure with phonon replicas at about 1.27 eV, which was attributed to a donor-acceptor pair (DAP) formed by the acceptor $\mathrm{Au_{Cd}}$ and an unknown donor. The peak at 1.576 eV was in both works connected with the shallow acceptor $\mathrm{Au_{Cd}}$. In this work, both appeared emissions were observed in samples without any Au doping or surface deposition during and between annealing steps, and a connection of both emissions with $\mathrm{Au_{Cd}}$ is questionable.

Recently, the same emission at 1.26 eV with a distinct phonon replicas structure was also observed in In-doped CdTe crystals annealed in Te vapor [19]. Since the emission is located in CdTe:Cl and CdTe:In at the same position, the origin of the emission is not connected with the type of a doping donor (Cl or In). The character of the emission at 1.26 eV was investigated on samples annealed under various Te pressure to study, whether the emission is formed by native defects. However, no dependence on the applied Te pressure was found. To conclude, the emission at 1.26 eV with the phonon replica structure can be attributed to a DAP defect with unclear composition. The origin of the peak at 1.576 eV can be assigned to an unknown bound

TABLE I
THE RESISTIVITY AND $\mu\tau$-PRODUCT OF ELECTRONS OF SAMPLES BEFORE AND AFTER TWO-STEP ANNEALING

	Resistivity (Ωcm) as-grown	$\mu\tau_e$ (cm^2/V) as-grown	Resistivity (Ωcm) after two-step annealing	$\mu\tau_e$ (cm^2/V) after two-step annealing
VGF-3	2×10^9	2.8×10^{-4}	2×10^9	2.7×10^{-4}
THM	2×10^9	2.8×10^{-3}	8×10^8	1.5×10^{-4}

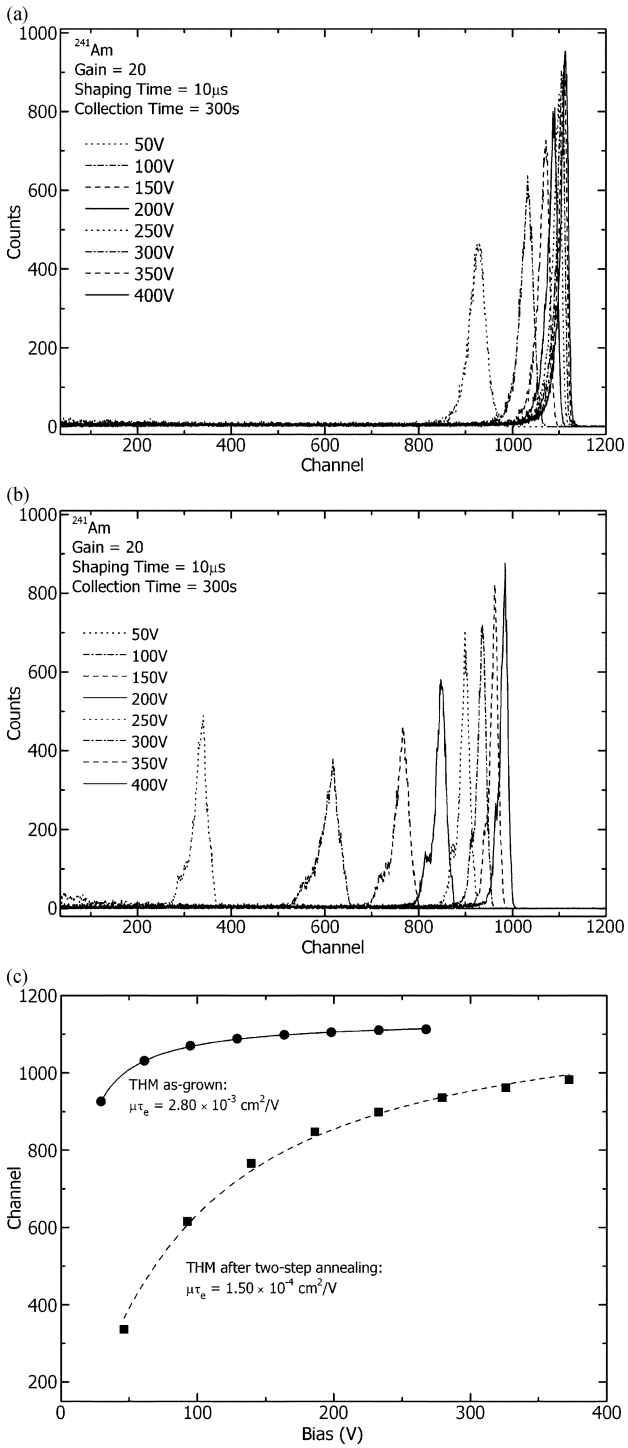

Fig. 8. Typical alpha-particle spectra of THM sample (a) before and (b) after two-step annealing. (c) Represents a Hecht analysis of the samples plotted on Fig. 8(a) and Fig. 8(b), respectively.

exciton or to the phonon replica of free exciton FE-LO usually observed at 1.575 eV.

E. Gamma-Ray and Alpha-Particle Spectra

Gamma-ray and alpha-particle spectroscopy of VGF-3 and THM crystals were performed before and after two-step annealing treatment. In γ-ray spectra of the VGF-3 crystal, the main photopeak was shifted to lower energies (Fig. 6). Observed high noise at low energies was caused by a significant surface leakage current. The $(\mu\tau)_e$ remained practically unchanged at a level of $2.7\times10^{-4}\ \mathrm{cm}^2/\mathrm{V}$ (see Table I). The main photopeak in γ-ray spectra of annealed THM samples was also shifted to lower energies and its FWHM increased (Fig. 7). Moreover, a significant drop of the $(\mu\tau)_e$ from $2.8\times10^{-3}\ \mathrm{cm}^2/\mathrm{V}$ to $1.5\times10^{-4}\ \mathrm{cm}^2/\mathrm{V}$ was observed (Fig. 8). In both crystals two effects can affect the detection ability after application of a two-step annealing: a) redistribution of impurities from Te inclusions during Cd-rich annealing and b) contamination of the material during the annealing treatment. Both effects could lead to incorporation of impurities into the crystal lattice and formation of an unknown deep level, which is not possible to seen in PL spectra and which markedly decreases the CCE. It is expected that the THM wafer was prepared from purer (7N) starting materials comparing to the VGF crystal (6N starting materials). Hence, the described effects had probably bigger influence on the detection ability of THM samples than of VGF-3 samples. In addition, it is expected that the CCE is not affected by the defect with the emission line at 1.26 eV found by PL, because this defect assigned to DAP is attributed to too shallow defects.

IV. CONCLUSIONS

An influence of a two-step post-growth annealing on the morphology of second phase defects and resistivity of CdTe:Cl was investigated. It was found that Cd-rich annealing effectively reduces the size of Te inclusions and also significantly decreases the material resistivity. Hence, re-annealing of the crystal in a Te atmosphere was necessary for the resistivity restoration. The resistivity of crystals after two-step annealing depended mainly on the chlorine doping level of CdTe:Cl and only very weakly on the applied Te pressure during the second annealing step in a Te atmosphere. The highest resistivity above $\rho > 10^8\ \Omega\mathrm{cm}$ after two-step annealing was observed in crystals with chlorine doping levels above $10^{17}\ \mathrm{cm}^{-3}$. Two models explaining obtained results were proposed and discussed. Moreover, two emissions at 1.26 eV and 1.576 eV were appeared in photoluminescence spectra after two-step annealing. However, the origin of the appeared peaks remains unclear. γ-ray spectra of annealed VGF-3 saples exhibited worse parameters comparng to as-grown samples. Contrary to this, the $(\mu\tau)_e$ was not much affected by the two-step annealing process. γ-ray spectra of the annealed THM crystal exhibited much worse parameters comparing to the as-grown crystal and the $(\mu\tau)_e$-product also significantly decreased after two-step annealing.

REFERENCES

[1] G. A. Carini, A. E. Bolotnikov, G. S. Camarda, G. W. Wright, R. B. James, and L. Li, "Effect of Te precipitates on the performance of CdZnTe detectors," *Appl. Phys. Lett.*, vol. 88, p. 143515, 2006.

[2] E. Belas, M. Bugár, R. Grill, P. Horodyský, R. Fesh, J. Franc, P. Moravec, Z. Matěj, and P. Höschl, "Elimination of inclusions in (CdZn)Te substrates by post-grown annealing," *J. Electron. Mater.*, vol. 36, no. 8, pp. 1025–1030, 2007.

[3] E. Belas, M. Bugár, R. Grill, J. Franc, P. Moravec, P. Hlídek, and P. Höschl, "Reduction of inclusions in (CdZn)Te and CdTe:In single crystals by post-growth annealing," *J. Electron. Mater.*, vol. 36, no. 9, pp. 1212–1218, 2008.

[4] M. Ayoub, M. Hage-Ali, A. Zumbiehl, R. Regal, J. M. Koebel, C. Rit, P. Fougeres, and P. Siffert, "Study of the resistivity mapping in CdTe:Cl—Correlation with annealing and Te precipitates," *IEEE Trans. Nucl. Sci.*, vol. 49, no. 4, pp. 1954–1959, Aug. 2002.

[5] M. Ayoub, M. Hage-Ali, J. M. Koebel, A. Zumbiehl, F. Klotz, C. Rit, R. Regal, P. Fougeres, and P. Siffert, "Annealing effects on defect levels of CdTe:Cl materials and the uniformity of the electrical properties," *IEEE Trans. Nucl. Sci.*, vol. 50, no. 2, pp. 229–237, Apr. 2003.

[6] R. Stibal, M. Wickert, P. Hiesinger, and W. Jantz, "Contactless mapping of mesoscopic resistivity variations in semi-insulating substrates," *Mater. Sci. Eng. B*, vol. 66, pp. 21–25, 1999.

[7] M. Ohmori, Y. Iwase, and R. Ohno, "High quality CdTe and its application to radiation detectors," *Mater. Sci. Eng. B*, vol. 16, pp. 283–290, 1993.

[8] B. K. Meyer and W. Stadler, "Native defects identification in II-VI materials," *J. Cryst. Growth*, vol. 161, pp. 119–127, 1996.

[9] G. Yang, A. E. Bolotnikov, Y. Cui, G. S. Camarada, A. Hossain, and R. B. James, "Impurity gattering effect of Te inclusions in CdZnTe single crystals," *J. Cryst. Growth*, vol. 311, pp. 99–102, 2008.

[10] R. Grill and A. Zappettini, "Point defects and diffusion in cadmium telluride," *Progr. Cryst. Growth Char. Mater.*, vol. 48, no. 9, pp. 209–244, 2004.

[11] P. Rudolph, "Non-stoichiometry related defects at the melt growth of semiconductor compound crystals—A review," *Cryst. Res. Technol.*, vol. 38, no. 7–8, pp. 542–554, 2003.

[12] E. Belas, M. Bugár, R. Grill, J. Franc, P. Moravec, P. Hlídek, and P. Höschl, "Preparation of inclusion and precipitate free semi-insulating CdTe," *IEEE Trans. Nucl. Sci.*, vol. 56, no. 4, pp. 1758–1762, Aug. 2009.

[13] M. A. Berding, "Native defects in CdTe," *Phys. Rev. B*, vol. 60, no. 12, pp. 8943–8950, 1999.

[14] R. F. Brebrick, "Equilibrium contacts for quasi-chemical reactions," *J. Elektron. Mater.*, vol. 33, no. 11, pp. L24–L26, 2004.

[15] R. Grill, P. Fochuk, J. Franc, B. Nahlovskyy, P. Höschl, P. Moravec, Z. Zakharuk, Y. Nykonyuk, and O. Panchuk, "High-temperature defect study of tellurium-enriched CdTe:In," *Phys. Stat. Sol. (b)*, vol. 243, pp. 787–793, 2006.

[16] R. Triboulet and P. Siffert, *CdTe and Related Compounds; Physics, Defects, Hetero- and Nano- Structures, Crystal Growth, Surfaces and Applications—Part I: Physics, CdTe-Based Nanostructures, CdTe-Based Semimagnetic Semiconductors, Defects*. New York: Elsevier, 2010, 978-0-08-046409-1.

[17] J. Hamann, A. Burchard, M. Deicher, T. Filz, V. Ostheimer, F. Strasser, H. Wolf, and T. Wichert, ISOLDE Collaboration, "Luminescence and influence of defect concentration on excitons in 197Hg/197Au-doped CdTe," *Physica B*, vol. 273–273, pp. 870–874, 1999.

[18] E. Molva, J. M. Francou, J. L. Pautrat, K. Saminadayar, and L. S. Dang, "Electrical and optical properties of Au in cadmium telluride," *J. Appl. Phys.*, vol. 56, no. 8, pp. 2241–2249, 1984.

[19] J. Procházka, E. Belas, R. Fesh, J. Franc, and P. Hlídek, "Photoluminescence of deep level complexes in CdTe," *Nucl. Instrum. Methods Phys. Res. A*, Jun. 18, 2010, 0168-9002.